JOURNAL OF NEUROTRAUMA 27:473–481 (March 2010)

DOI: 10.1089/neu.2009.1058

Metabolic Levels in the Corpus Callosum and Their Structural and Behavioral Correlates after Moderate to Severe Pediatric TBI

Talin Babikian,[1] Sarah DeBoard Marion,[2] Sarah Copeland,[3] Jeffry R. Alger,[4,5] Joseph O'Neill,[1] Fabienne Cazalis,[1] Richard Mink,[6] Christopher C. Giza,[3,9] Jennifer A. Vu,[7] Suzanne M. Hilleary,[2] Claudia L. Kernan,[1] Nina Newman,[1] and Robert F. Asarnow[1,8]

Abstract

Diffuse axonal injury (DAI) secondary to traumatic brain injury (TBI) contributes to long-term functional morbidity. The corpus callosum (CC) is particularly vulnerable to this type of injury. Magnetic resonance spectroscopy (MRS) was used to characterize the metabolic status of two CC regions of interest (ROIs) (anterior and posterior), and their structural (diffusion tensor imaging; DTI) and neurobehavioral (neurocognitive functioning, bimanual coordination, and interhemispheric transfer time [IHTT]) correlates. Two groups of moderate/severe TBI patients (ages 12–18 years) were studied: post-acute (5 months post-injury; $n = 10$), and chronic (14.7 months post-injury; $n = 8$), in addition to 10 age-matched healthy controls. Creatine (energy metabolism) did not differ between groups across both ROIs and time points. In the TBI group, choline (membrane degeneration/in-inflammation) was elevated for both ROIs at the post-acute but not chronic period. N-acetyl aspartate (NAA) (neuronal/axonal integrity) was reduced initially for both ROIs, with partial normalization at the chronic time point. Posterior, not anterior, NAA was positively correlated with DTI fractional anisotropy (FA) ($r = 0.88$), and most domains of neurocognition (r range 0.22–0.65), and negatively correlated with IHTT ($r = -0.89$). Inverse corerlations were noted between creatine and posterior FA ($r = -0.76$), neurocognition (r range -0.22 to -0.71), and IHTT ($r = 0.76$). Multimodal studies at distinct time points in specific brain structures are necessary to delineate the course of the degenerative and reparative processes following TBI, which allows for preliminary hypotheses about the nature and course of the neural mechanisms of subsequent functional morbidity. This will help guide the future development of targeted therapeutic agents.

Key words: corpus callosum; diffusion tensor imaging; evoked potentials; magnetic resonance spectroscopy; pediatric traumatic brain injury

Introduction

Diffuse axonal injury (DAI) caused by traumatic brain injury (TBI) plays a major role in subsequent long-term functional morbidity. Conventional diagnostic computed tomography and magnetic resonance imaging (MRI), however, often do not detect subtle DAI, and therefore do not provide an explanation for lingering neurological or neurobehavioral symptoms (Ashwal et al., 2006b; Meythaler et al., 2001; Tasker et al., 2006). Consequently, more sensitive imaging techniques are needed to not only improve prognostic ability (Ashwal et al., 2006a), but also to elucidate the underlying neural mechanisms that explain neurological and neurocognitive deficits, and the restorative and repair processes that follow.

Contrary to nomenclature, DAI is not necessarily diffuse, but is rather multifocal, leading some to use the term

[1]Departments of Psychiatry and Biobehavioral Sciences, [3]Neurosurgery, [4]Neurology, and [5]Radiological Sciences, and [9]Pediatrics, David Geffen School of Medicine, University of California–Los Angeles, Los Angeles, California.
[2]Department of Psychology, Fuller Graduate School of Psychology, Pasadena, California.
[6]Department of Pediatrics, David Geffen School of Medicine at UCLA and Los Angeles Biomedical Research Institute at Harbor-UCLA, Los Angeles, California.
[7]UCLA Graduate School of Education and Information Studies, University of California–Los Angeles, Los Angeles, California.
[8]Department of Psychology, UCLA Graduate School, Los Angeles, California.

traumatic axonal injury instead (Gorrie et al., 2002). Histopathologically, DAI is characterized by widespread damage to the axons of the brainstem, parasagittal white matter of the cerebrum, corpus callosum (CC), and the gray-white junctions of the cerebral cortex (Meythaler et al., 2001), with greatest involvement in the frontal white matter, brainstem, diencephalon, and the CC (Tong et al., 2004). As the largest white matter tract in the brain, the CC is particularly vulnerable to DAI. There are reductions in CC volume following pediatric TBI, with continuing degeneration over time in more severe injuries (Levin et al., 2000). On MRI studies, approximately 25% of children showed CC injury following TBI, particularly in the posterior body and splenium (Wilde et al., 2006). Diffusion tensor imaging (DTI) studies in children after TBI have shown decreases in fractional anisotropy (FA) in the CC and its associated fibers (Akpinar et al., 2007; Ewing-Cobbs et al., 2006; Wilde et al., 2006; Yuan et al., 2007), a measure that reflects directionality of water diffusion and is interpreted as a marker of white-matter integrity. FA values in the CC have also correlated with injury severity (e.g., Glasgow Coma Scale [GCS] scores), (Yuan et al., 2007) and functional outcomes (Ewing-Cobbs et al., 2006; Wilde et al., 2006).

In addition to structural changes, there is a neurochemical and metabolic cascade initiated by TBI that contributes to functional morbidity. Magnetic resonance spectroscopy (MRS) provides non-invasive quantifiable metabolic measures of neuronal/axonal integrity (N-acetyl aspartate or NAA), energetic metabolism (creatine or Cre), and membrane breakdown and/or inflammation (choline or Cho), as well as other indicators of cellular function and dysfunction (Ashwal et al., 2000, 2006b; Hoon and Melhem, 2000). MRS studies of pediatric TBI (accidental and other injuries) during the acute stage (the first 2 weeks) show elevations in lactate (Ashwal et al., 2000; Sutton et al., 1995) and Cho, and reductions in NAA, which predict poor gross neurological functioning at 6 months post-injury (Ashwal et al., 2000; Holshouser et al., 2000), and poor long-term (>1 year) neurocognitive outcomes (Babikian et al., 2006; Brenner et al., 2003). At longer post-injury intervals (up to 5 months), there are reductions in NAA and elevations in Cho in both the anterior and the posterior white and gray matter, which correlate with language and visuomotor functioning (Yeo et al., 2006). Reductions in NAA and Cho in the right frontal lobe 1–12 years post-injury predict poor neuropsychological outcome (Parry et al., 2004). Similarly, NAA reductions in the medial frontal gray matter correlate with neurobehavioral measures 1–3 years post-injury (Walz et al., 2008). Further, although lower NAA levels from predominantly white matter regions 6 weeks to 3 years post-injury predict neurocognitive functioning, no differences between children with TBI and controls in Cho in the same regions are noted (Hunter et al., 2005).

Despite the vulnerability of the CC to DAI, little is known about changes in brain metabolites specifically in this region following TBI, including the time course of metabolite abnormalities following an injury, its correlation with structural measures of white matter integrity, or functional measures of the CC. The goals of this study were twofold: (1) to test the hypothesis that post-acutely, pediatric TBI patients show reductions in CC NAA and elevations in CC Cho compared to age-matched healthy controls, and that these differences in neurometabolism diminish at 1 year post-injury (when substantial functional recovery has occurred); and (2) to examine the structural (DTI) and functional (electrophysiological and neurobehavioral) correlates of metabolite changes in the CC following a moderate to severe injury in order to determine the degree to which multimodal imaging and its behavioral correlates collectively advance our knowledge and generate insights into neural injury and repair mechanisms following pediatric TBI. The ultimate motivation of this work is to guide targeted therapeutic agents.

Methods

Patients recruited from pediatric intensive care units in Los Angeles County (UCLA Medical Center and Harbor-UCLA Medical Center) and the Centre for Neuro Skills, a rehabilitation hospital, were included in this study if they met the following criteria: (1) moderate to severe non-penetrating TBI (intake or post-resuscitation GCS score between 3 and 12, or higher GCS score with confirmed abnormalities on clinical imaging); (2) 8–18 years of age at injury; (3) normal visual acuity or vision corrected with contact lenses/eyeglasses; and (4) English skills sufficient to understand instructions and participate in the neurocognitive measures. Patients with a pre-trauma history of neurological, developmental, or psychiatric disorders (including prior head injury) or MR-incompatible metal implants were excluded.

A total of 25 subjects underwent MRS scanning. These included 15 TBI patients and 10 healthy controls. TBI patients were divided into a "post-acute" group (on average 5 months post-injury; $n = 10$), and a "chronic" group (on average 14.7 months post-injury; $n = 8$) (Table 1). Table 2 contains case-by-case demographic and clinical information for the post-acute TBI group. Three of the patients in the post-acute group were evaluated a second time and were included in the eight subjects of the chronic group. The remaining five in the chronic group were recruited later and participated only at the chronic time point. The same healthy control group was compared to both the post-acute and the chronic groups, with the exception of one older healthy control subject who was included in the chronic analyses but not in the post-acute analyses so that the groups would be better matched by age. These 10 controls were age-matched to the post-acute group, but were significantly younger than the chronic group (Table 1). Therefore, all of the statistical analyses involving comparisons between the chronic and control groups were repeated controlling for age, although no statistically significant age-related effects were noted. Controls had no history of head trauma and satisfied criteria 2–4 above. Participants underwent neuroimaging, electrophysiological, and behavioral evaluations on the same day, or on rare occasions, within at most a 2-week span. Although all subjects underwent MRS scanning and behavioral testing, only four subjects (all in the post-acute TBI group) underwent electrophysiological assessment.

Behavioral measures

Neurocognitive tests. The following functional domains were assessed: (1) general intellectual functioning using the Full Scale IQ (FSIQ) score from the Wechsler Abbreviated Intelligence Scale (WASI) (Wechsler, 1999); (2) verbal memory using the age standardized Immediate Memory Total score from the California Verbal Learning Test–Second Edition (CVLT-II) or Children's Version (CVLT-C), depending on age (Delis et al., 1994, 2000); (3) visual memory using standard

Table 1. Mean (SD) and Independent Samples *t*-Test Results for the Groups by Time Point Post-Injury for the Anterior and Posterior Callosal Sections

Post-acute	*TBI* (n = *10*)	*Control* (n = *10*)
Gender	8 Male	5 Male
Age (years) at assessment	15.6 (1.7)	14.4 (2.01)
Time post-injury (months)	5.2 (1.5)	N/A
GCS	8.6 (4.8)	N/A
GM (%) (A)	.24 (.10)	.30 (.14)
(P)	.12 (.05)	.20 (.19)
WM (%) (A)	.72 (.09)	.70 (.10)
(P)	.83 (.06)	.81 (.07)
CSF (%) (A)	.03 (.04)	.02 (.02)
(P)	.05 (.05)	.05 (.03)
Number of voxels		
(A)	5.46 (3.1)	4.27 (3.2)
(P)	11.3 (2.2)	10.0 (3.6)
Chronic	*TBI* (n = *8*)	*Control* (n = *10*)
Gender	7 Male	5 Male
Age (years) at assessment	17.9 (.97)	15.3 (1.88)*
Time post-injury (months)	14.7 (2.34)	N/A
GCS	8.0 (5.4)	N/A
GM(%) (A)	0.23 (0.12)	0.30 (0.14)
(P)	0.16 (0.04)	0.19 (0.19)
WM(%) (A)	0.72 (0.14)	0.70 (0.11)
(P)	0.77 (0.07)	0.82 (0.07)
CSF(%) (A)	0.04 (0.05)	0.02 (0.02)
(P)	0.07 (0.05)	0.04 (0.03)
Number of Voxels		
(A)	3.45 (2.4)	4.3 (3.2)
(P)	9.90 (2.5)	10.0 (3.6)

A, anterior corpus callosum; P, posterior corpus callosum; GCS: Glasgow Coma Scale score; TBI, traumatic brain injury; GM/WM/CSF, average percentage of tissue content (gray matter, white matter, or cerebrospinal fluid, respectively) in voxels reported in the analyses.
*$p < 0.05$.

scores for the Faces subtests from the Wechsler Memory Scale–Third Edition (WMS-III) or Children's Memory Scale (CMS), depending on age (Cohen, 1997; Wechsler, 1997); (4) psychomotor processing speed using the Processing Speed Index of the Wechsler Adult Intelligence Scale–Third Edition (WAIS-III) or Wechsler Intelligence Scale for Children–Fourth Edition (WISC-IV), depending on age (Wechsler, 1997, 2003); and (5) attention span/working memory using the Working Memory Index of the appropriate Wechsler Intelligence Scale (Wechsler, 1997, 2003).

Behavioral measure of CC function. Participants performed the computerized Bimanual Coordination Test (BMCT) (Brown, 1991). On this test, participants are required to maneuver a cursor on a computer monitor along rectilinear target pathways oriented at various angles using an "Etch-a-Sketch®"-style response box. The measures collected from the BMCT include: (1) response latency or time to complete a trial, and (2) response accuracy measured by the degree of deviation from a perfect linear response. The BMCT assesses three aspects of motor coordination: (1) pure motor speed, measured by the time taken to complete right- and left-hand unimanual trials; (2) general visuomotor coordination, measured by the speed and accuracy of angles requiring equal or symmetric hand speed; and (3) interhemispheric cooperation, measured by speed and accuracy of angles requiring unequal or asymmetric hand speed. Additional bimanual trials completed without visual input halfway through the trial demand further callosal input, making the asymmetric trials completed without visual control the most demanding of interhemispheric communication and callosal integrity (DeBoard Marion et al., 2008). The BMCT has been shown to require more anterior CC connections between premotor brain regions (Jeeves et al., 1988; Preilowski, 1972).

Electrophysiological measure

Interhemispheric transfer time (IHTT). We used visual event-related potentials (ERPs) to measure the transfer of stimulus-locked neural activity between the hemispheres in four patients. ERPs were collected during a computerized bilateral field advantage task. Following a gaze-fixation (a colon) in the center of the visual field, participants were exposed to two distinct visual stimuli (geometric shapes made by patterns of 9- to 11-letter "o"s) presented tachistoscopically and randomly to two of the four visual fields (upper and lower; left and right). This created two unilateral conditions (right and left visual fields; RVF and LVF), and four bilateral conditions. Electroencephalographic (EEG) visual ERPs collected during the unilateral conditions were used to calculate

Table 2. Characteristics of the Patient Sample Included in the Correlational Analyses (Post-Acute Studies)

Case	*Time post-injury (months)*	*Visible CC lesions*	*Gender*	*Age at injury (years)*	*GCS*	*Injury mechanism*
1	3	None	M	15.8	14	Fall
2	4	None	M	16.3	11	MVA
3	5	Posterior	M	17.4	3	MVA
4	5	Middle and posterior	M	16.0	5	MVA
5	6	None	M	12.1	12	Boat
6	4	None	M	16.1	5	MVA
7	5	None	M	13.2	3	MVA
8	4	None	F	17.6	15	Assault
9	7	Mid	M	15.0	5	Ped/Auto
10	8	Mid and Anterior	F	16.2	13	MVA

CC, corpus callosum; GCS, Glasgow Coma Scale score; MVA, motor vehicle accident; Ped/Auto, pedestrian/automobile accident.

each participant's cross-callosal interhemispheric transfer time (IHTT). This is calculated by averaging EEG waveforms at the P1 (left hemisphere) and P2 (right hemisphere) electrode sites, identifying the peak latency (msec) of the early N1 evoked potential components, and then subtracting the latencies of the ipsilateral and contralateral conditions. The longest IHTT (RVF-LVF or LVF-RVF) was used in the remaining analyses. This procedure is described in greater detail elsewhere (DeBoard Marion et al., 2008). IHTT is sensitive to disruptions of the CC (Brown et al., 1999; Rugg et al., 1985), as demonstrated in patients with commissurotomies, callosotomies, and callosal agenesis. Longer IHTTs indicate slower transfer of information across the posterior visual brain regions.

Brain imaging

Structural MRI methods. All images were acquired at the UCLA Ahmanson-Lovelace Brain Mapping Center using a Siemens 1.5 T Sonata MR scanner. The MPRAGE Siemens pulse sequence (flip angle = 15°, TR = 1900 msec; TE = 4.38 msec; FoV = $1.0\times1.0\times1.0$ mm^3; 160 slices, 1 mm/slice, no gaps) was used to obtain high-resolution sagittal structural volumetric scans of the entire brain. Two acquisitions were performed and the results were co-registered and averaged together off-line. This yielded 1-mm isotropic voxels with excellent T1 contrast.

MRSI methods. Multi-voxel MRS, or magnetic resonance spectroscopic imaging (MRSI), of the brain was performed at the same session as MRI, using the PRESS-CSI Siemens product sequence (TR = 1500 msec; TE = 135 msec; NEX = 4; 16×16 phase-encoding resolution with Hamming filter; FoV = 160×160 mm^2; slice thickness = 10 mm; acquisition time = 7.5 min). MRSI was acquired from an axial-oblique slice sampling the corpus callosum. Using the scout and the sagittal MPRAGE, the CC slice was aligned parallel to the AC/PC plane and positioned with its inferior surface a few millimeters above the roof of the lateral ventricles. Slice location, slice angulation, and PRESS volume selection were adjusted for each subject to maximize inclusion of the CC within the sampled volume. Note that the dimensions of the PRESS volume were further constrained to remain within the brain in order to minimize contamination of the spectra with extracranial lipid signals. Adjustments of magnetic field homogeneity (shimming), water suppression, and transmitter power were performed using the manufacturer's automated pre-scan software. Intermediate TE (135 msec) was used rather than short TE because we have found that longer TE acquisitions have substantially better data quality for the target metabolite signals (NAA, Cr, and Cho). There are substantially fewer artifacts due to inadequate water and lipid suppression at TE = 135 compared to TE = 30 msec.

MRSI spectra were fit off-line using the LCModel commercial software package (Provencher, 2001). LCModel yielded NAA, Cr, and Cho levels for each spectroscopic voxel in the CC MRSI slice. Voxels located on the edges of the PRESS-select volume were discarded because the metabolite signal intensities in these voxels are distorted by the volume selection procedure. To correct for partial-volume effects of voxel CSF content, the MPRAGE whole-brain MRI volume was tissue-segmented into gray matter, white matter, and CSF using the Statistical Parametric Mapping (SPM) software package (http://www.fil.ion.ucl.ac.uk/spm/). The resulting gray matter, white matter, and CSF whole-brain volumes were then co-registered with the callosal MRSI slice, and the volume fraction gray matter, white matter, and CSF in each spectroscopic voxel was identified using the MRSI Voxel Picker (MVP) program developed at UCLA (O'Neill et al., 2006). The voxel levels of NAA, Cr, and Cho obtained from LCModel (see below) were then normalized to one minus the volume fraction CSF to put these metabolite measures on a per-tissue-volume basis. The MVP-guided user interface, which displayed the MRSI grid atop the co-registered MPRAGE structural MRI, enabled us to pick MRSI voxels within two regions of interests (ROIs). These were defined as the anterior CC and adjacent white matter fibers, and the posterior CC and adjacent white matter fibers. Voxels from the mid-section of the CC were excluded so that the voxels selected would be clearly anterior or posterior. Automated quality control criteria for voxels within the ROIs enforced by MVP were: (1) at least 50% white matter; (2) full width at half maximum (FWHM) < 0.1 ppm; and (3) signal-to-noise ratio (S/N) ≥ 2. Voxels not meeting these criteria were rejected from the analysis. Additionally, individual metabolite peaks were rejected if they did not satisfy the LCModel criterion of $< 20\%$ standard deviation. These automated criteria were supplemented by operator inspection of each spectrum as prescribed in the LCModel manual. Using these quality-control procedures, the number of voxels retained in each ROI ranged from 1–15 across subjects. Representative values of NAA, Cr, and Cho were obtained by averaging the values for all voxels retained across each ROI for each subject.

DTI methods. Whole-brain DTI was acquired using the pulse sequence developed for the International Consortium for Brain Mapping. Briefly, echo-planar DTI (TR = 6400 msec; TE = 83 msec; FoV = 240 mm; slice thickness = 2.5 mm) was acquired in an axial-oblique orientation parallel to the AC/PC plane. The Jones-30 direction diffusion-sensitization scheme with five repeats of the b = 0 image acquisition was used (Jones, 2004). DTI raw data were post-processed using SPM software, resulting in whole-brain FA maps. Additionally, the mean FA was computed across whole-brain white matter and the CC, as well as the ROIs within the CC (anterior and posterior). The specifics of DTI acquisition and processing are described elsewhere (Copeland et al., 2008).

Statistical analyses

Analyses reported include independent samples *t*-tests and Pearson correlations. Considering the small sample size in the study, non-parametric equivalents of the above statistics were also used in all instances, with no notable differences observed in the outcomes reported. Therefore, only the parametric statistics will be reported below.

Results

Using cross-sectional data, patients were imaged on average 5.2 months post-injury in the post-acute studies and 14.7 months post-injury for the chronic studies (Table 1). Based on post-acute MPRAGE sequences, two of the TBI patients showed visible lesions in the posterior CC, one showed a

lesion in the mid-body of the CC, and another showed lesions on both the mid-body and anterior CC sections. At the chronic time point, two of the patients showed visible lesions in the posterior CC, and one showed a lesion in the posterior and mid-body of the CC.

MRSI (post-acute and chronic)

There were no differences in voxel tissue content (gray and white matter, or CSF) between TBI patients and controls for the post-acute or chronic groups, in either the anterior or posterior CC ROIs. For both the post-acute and chronic groups, mean anterior and posterior CC white-matter content was at least 70% (Table 1). Further, in the post-acute TBI group, there were no differences from controls in either anterior or posterior CC on measures of spectral quality (S/N ratio and FWHM). In the chronic group, posterior FWHM was higher in patients, while both anterior and posterior S/N ratios were lower in the TBI group ($p < 0.05$). In both the TBI and control groups, white-matter content was higher in the posterior than in the anterior CC for the post-acute and chronic groups. Posterior white-matter content of the chronic group was higher in the control group ($p = 0.02$) (Table 1).

There were no statistically significant group differences between the post-acute or chronic TBI and control groups in either anterior or posterior CC Cre. Further, Cre levels did not differ between the post-acute and chronic TBI groups in either ROI (Fig. 1). In the post-acute and chronic TBI groups, and in the control groups, NAA was higher in the posterior than in the anterior CC, with these differences statistically significant ($p < 0.01$ or less) for all comparisons except in the chronic TBI group ($p = 0.51$). NAA was significantly lower in the anterior CC in the post-acute TBI group ($p = 0.03$), and in the posterior CC in the chronic TBI group ($p = 0.04$), compared to their respective control groups. Group differences approached significance for the anterior CC in the chronic TBI group ($p = 0.09$). There were no differences in NAA levels between the post-acute and chronic TBI groups in either ROI (Fig. 2).

Within groups, no differences in anterior versus posterior CC Cho were observed. Of note, however, Cho was significantly elevated in the posterior CC ROI in the post-acute TBI group ($p = 0.02$), but not in the chronic TBI group ($p = 0.69$). Elevations in Cho in the anterior CC in the post-acute TBI group approached significance ($p = 0.09$), but no group differences were observed at the chronic time point ($p = 0.58$) (Fig. 3).

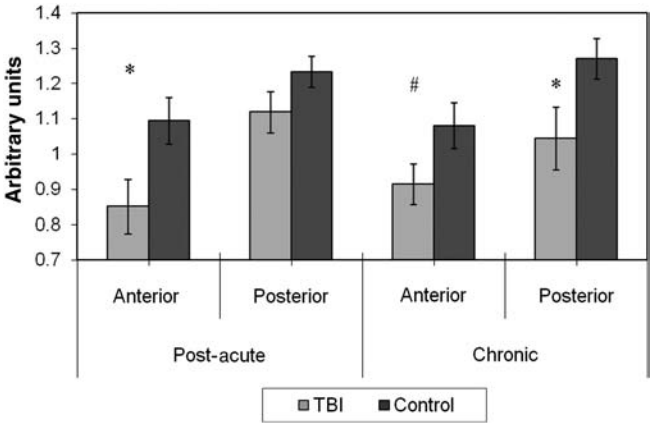

FIG. 2. Post-acute and chronic anterior and posterior callosal N-acetyl aspartate (NAA) by group (*$p < 0.05$; #$p < 0.10$).

Correlations between MRSI and measures of CC structure and function (post-acute only)

Pearson correlation coefficients were calculated for the associations between MRSI metabolite concentrations in the CC and the following structural and neurobehavioral callosal functional measures for the post-acute time point (TBI patients only), since the sample with multimodal evaluations in the chronic period was too small to report.

Glasgow Coma Scale (GCS) score. There were no statistically significant correlations between anterior CC metabolites and GCS scores. However, a positive association between posterior CC NAA, and a negative association (showing a statistical trend) between posterior CC Cho were observed (Table 3).

DTI fractional anisotropy (FA). The anterior CC metabolite concentrations were not correlated significantly with either anterior or posterior callosal FA. While posterior CC Cre was not correlated with FA, there were several strong correlations between other posterior CC metabolites and FA. Specifically, NAA was positively correlated with callosal FA, particularly in the posterior CC region. In contrast, Cho was negatively

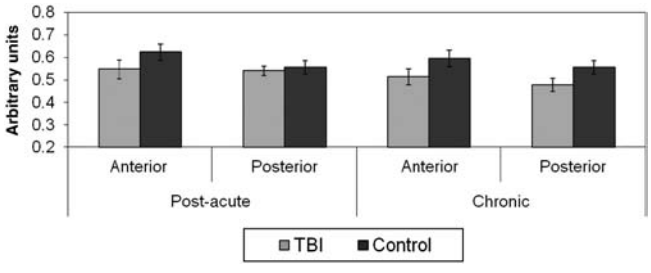

FIG. 1. Post-acute and chronic anterior and posterior callosal creatine (Cre) by group. No statistically significant group differences were present.

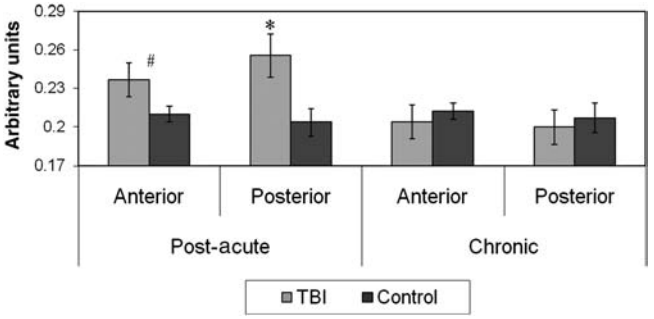

FIG. 3. Post-acute and chronic anterior and posterior callosal choline (Cho) by group (*$p < 0.05$; #$p < 0.10$).

Table 3. Pearson Correlation Coefficients Between MRS Metabolites and Structural, Neurobehavioral, and Electrophysiological Measures of the Corpus Callosum (CC) for the Post-Acute TBI Group

	Anterior CC			*Posterior CC*		
	NAA	*Cre*	*Cho*	*NAA*	*Cre*	*Cho*
GCS	0.152	−0.356	−0.561	0.908*	0.104	−0.587#
Whole brain FA	0.102	0.189	0.064	0.466	0.284	−0.417
Anterior CC FA	0.633	−0.028	0.057	0.695	−0.473	−0.879*
Posterior CC FA	0.144	−0.376	−0.393	0.881*	−0.098	−0.757*
Verbal memory	−0.059	0.013	0.013	0.429	0.025	−0.218
Visual memory	0.394	−0.142	−0.150	0.651*	−0.124	−0.713#
FSIQ	0.355	−0.092	0.035	0.630*	−0.134	−0.490*
PSI	0.245	−0.216	−0.164	0.567*	−0.244	−0.434
WMI	0.086	0.330	0.385	0.220	−0.376	−0.146
IHTT ($n = 4$)	0.125	0.213	0.196	−0.885*	0.732*	0.755*
BMCT						
Time_Symm	0.044	0.716*	0.668*	−0.334	−0.199	0.169
Time_Asymm	0.313	0.325	0.386	0.372	0.191	−0.308
Error_Symm	0.346	−0.150	0.032	−0.177	0.209	−0.077
Error_Asymm	0.063	−0.416	−0.061	−0.402	0.511	0.232

*$p < 0.05$; #$p < 0.10$.

GCS, Glasgow Coma Scale score; NAA, N-acetyl aspartate; Cre, creatine; Cho, choline; FA, fractional anisotropy; FSIQ, Full Scale IQ; PSI, Processing Speed Index; WMI, Working Memory Index; ERP, event-related potential; IHTT, Interhemispheric Transfer Time from ERP paradigm; BMCT, Bimanual Coordination Test; TBI, traumatic brain injury.

Time_Symm and Time_Asymm refer to the time it took to complete the task for the combined symmetric and asymmetric angles, respectively. Error_Symm and Error_Asymm refer to the error (area of deviation from a straight line) associated with completing the task for the combined symmetric and asymmetric angles, respectively.

correlated with callosal FA (combined, as well as from the anterior and posterior regions independently) (Table 3).

Neurocognitive measures. Consistent with the DTI correlations above, anterior CC metabolite concentrations did not correlate significantly with any of the neurocognitive measures. No significant correlations between posterior Cre and any of the neurocognitive measures were also observed. On the other hand, positive correlations were noted between posterior CC NAA and several neurocognitive measures, reaching statistical significance for FSIQ, visual memory, and processing speed. Further, generally negative correlations were observed between posterior CC Cho and neurocognitive performance, which reached statistical significance for FSIQ, and approached significance for visual memory (Table 3).

Bimanual Coordination Test (BMCT; response time and error). Contrary to the pattern of correlations above, posterior CC metabolites did not correlate significantly with response time on the BMCT. Rather, anterior Cre and Cho (but not NAA) were positively correlated with the response time variable. Further, no correlations were observed between the anterior or posterior CC metabolite concentrations and the error variable on the BMCT (Table 3).

Interhemispheric transfer time (IHTT). The subset of our sample with both MRSI and ERP data was very small ($n = 4$). There were, nonetheless, intriguing preliminary findings that are worth mentioning and warrant replication. Similar to the above pattern of correlations, there were no meaningful correlations between anterior CC metabolite concentrations and IHTT. On the other hand, IHTT was inversely and significantly correlated with posterior CC NAA, and positively correlated with posterior CC Cho and Cre (Table 3).

Discussion

There is an emerging and fairly consistent body of literature showing brain metabolic abnormalities detected by MRS following pediatric TBI. Studies have shown reductions in NAA acutely (Ashwal et al., 2000; Holshouser et al., 2005), post-acutely, and years following more severe injuries (Parry et al., 2004; Walz et al., 2008), with these reductions predicting or correlating with neurological and/or neurocognitive outcomes (Babikian et al., 2006; Parry et al., 2004; Walz et al., 2008). Although not observed as consistently, elevations in Cho have also been reported, particularly in the early phases post-injury (Ashwal et al., 2000; Yeo et al., 2006). However, with one exception in which normalization in metabolites in a series of post-acute evaluations was shown (Yeo et al., 2006), there are no studies to date that assess how brain metabolic abnormalities evolve at discrete time points post-TBI that might reflect the time course of physiological recovery underlying functional improvement. Ideally, this would be studied longitudinally to control for between-subject variability (especially important in TBI research, where there is often a large degree of heterogeneity). Since longitudinal data are thus far not available, we presented cross-sectional data from discrete time points post-injury in this study to demonstrate the manner in which multimodal evaluations can potentially elucidate underlying mechanisms of injury and repair.

Time course of NAA and its structural and behavioral correlates

Reductions in callosal NAA compared to healthy controls were observed in both the post-acute (anterior CC) and chronic (posterior CC) TBI groups, indicating that brain metabolite abnormalities in axonal fibers and/or reduction in the

number of fibers per unit volume are present during the first year post-injury. These abnormalities could reflect long-term changes in energy metabolism or simply cell/axon loss. NAA reductions have been attributed to permanent cell death (in more severe injuries), an increased rate of NAA hydrolysis required to meet increased demands for the lipid synthesis involved in myelin repair, and to its role as a temporary source of cell energy at the site of axonal injury (Cecil et al., 1998; Holshouser et al., 2005; Ross et al., 1998). The persistent decrements in NAA seen in more severe injuries are distinct from those that occur following milder injuries, where complete normalization can be observed within the first month post-injury (Vagnozzi et al., 2008).

In this study, reduced post-acute posterior callosal NAA was strongly associated with reduced callosal FA (particularly the posterior FA) from DTI studies. Thus, low NAA and low FA may both be markers of impaired axonal integrity in the callosum in the post-acute period. The normal levels of Cho measured in the chronic TBI group suggest eventual cessation of early-phase post-traumatic membrane degenerative processes or proliferations in the inflammatory response, while the continuing deficits in NAA seen in the chronic TBI group suggest ongoing neuronal metabolic impairment and/or cell death at later stages post-insult (Holshouser et al., 2005). Further, increased levels of posterior callosal NAA were associated with better performance on neurocognitive measures of visual memory, general intelligence, and psychomotor processing speed and decreased IHTT. Although this study does not reveal the underlying causes of diminished NAA, such as neuronal death or hypometabolism, the association with low FA is suggestive of axonal pathology.

Time course of Cho and its structural and behavioral correlates

In our cross-sectional analyses, elevations in Cho were observed in post-acute TBI patients, but not in chronic TBI patients (three of whom were also included in the post-acute group). Post-traumatic Cho elevation has been described as the "second most common finding (after NAA depletion)" in head-injury research, and is attributed to the breakdown of myelin (axonal injury) and cellular membranes (gray matter/neuronal perikaryal injury), as well as inflammation following shearing injuries (Ross et al., 1998). The post-acute Cho elevation in white matter seen in this study may be a signal of demyelination and/or of an inflammatory response, including necrosis and repair/clean-up of myelin breakdown, consistent with previous reports (Ashwal et al., 2000; Yeo et al., 2006). As such, Cho may be considered a biomarker for *ongoing* pathological processes. This process, at least as detected by its MRS signal *in vivo*, was not observed in our chronic TBI group. Normalization of Cho by the chronic post-TBI stage would be consistent with prior literature showing no abnormalities in Cho (Hunter et al., 2005; Walz et al., 2008).

We found a negative correlation between post-acute DTI FA and posterior CC Cho. Although some normalization in FA from the post-acute to the chronic period has been evident in our studies (Copeland et al., 2008), persistent decreases in FA have been reported following the first year of injury (Akpinar et al., 2007; Wilde et al., 2006). To the extent that FA is a signal of axonal microstructural integrity (Arfanakis et al., 2002; Huisman et al., 2004; Wilde et al., 2006), its association with posterior callosal Cho in the post-acute period suggests that *in vivo*, Cho reflects structural changes (presumably inflammatory processes and demyelination) that follow traumatic axonal injury. On the other hand, the fact that normal Cho levels were observed chronically in conjunction with an improvement, but not complete normalization, of FA (presumably due to remyelination or other repair processes) over this same time course (Copeland et al., 2008) suggests that membrane breakdown ceases despite evidence for continued structural abnormalities reflected in the persistent low levels of NAA.

There were negative correlations post-acutely between posterior callosal Cho and behavioral measures of visual memory and general intellectual functioning. Elevations in Cho predicted poorer performance on measures of visual memory and general intellectual functioning. The posterior CC apparently connects parts of networks involved in these neurocognitive domains. These neurocognitive domains require a large range of cognitive sub-processes that require integrated activity of various brain structures both within and between the two hemispheres. Apparently elevated levels of Cho in the posterior CC reflect changes in CC function that disrupt transfer of information between the hemispheres. Although very preliminary due to the small sample subset ($n = 4$) of patients for whom both MRS and specific measures of callosal transfer time (IHTT) were available, it was noteworthy that post-acutely, elevated levels of Cho predicted slower transfer of information between the two hemispheres.

In contrast to many of the above findings in the posterior CC, it was *anterior* callosal Cho that correlated positively with the response time variable of the BMCT, a measure of bimanual coordination. This is consistent with the notion that the BMCT is largely a measure of anterior callosal function. The BMCT error variable was not correlated with callosal Cho levels in the anterior or posterior ROIs.

Detection of Cho well into the post-acute period shows ongoing metabolic dysfunction in more severe injuries and raises the possibility that Cho detected acutely and post-acutely may reflect different underlying mechanisms of cellular dysfunction. As such, it would be important to determine whether the presence of Cho *post-acutely* is a predictor of later functional outcome.

Anterior versus posterior findings

Although reductions in NAA and elevations in Cho were observed in both the anterior and posterior callosum, with the exception of the response time on the BMCT, we observed significant structure/function correlations in the posterior callosum only. The posterior CC, including the splenium, is particularly vulnerable to traumatic brain injury (Cecil et al., 1998; Gentry et al., 1988; Mendelsohn et al., 1992). The vulnerability of the posterior CC may make it a particularly informative region to study when examining the effects of DAI in brain-behavior correlation studies. In our study, at least in the post-acute TBI group for which correlational data were reviewed, there were no group differences in spectral quality or the tissue content of the voxels included in the analyses. Of note, however, in the TBI group, there was a higher average concentration of white matter in the posterior versus the anterior region (83% versus 72%, respectively). The signal-to-noise ratio (S/N) was also more favorable in the posterior

region compared to the anterior region (6.6 versus 4.5, respectively), although both met minimal requirements to assure spectral quality for voxel inclusion. Increased concentration of white matter and superior spectral quality in the posterior callosum may have contributed to more sensitive measurements of callosal function and dysfunction. This, however, is unlikely to be the sole explanation for the strong associations found within the posterior callosum given the extant literature on the vulnerability of this region to injury. Further, as indicated in the results section, relatively few of the patients had visible lesions on their radiologic studies, with both anterior and posterior CC lesions observed. Therefore, overt structural lesions and subsequent partial volume effects alone do not seem to fully explain the regional specificity of the correlational findings in this study.

Conclusions, limitations, and future directions

The primary limitations of this study were the small sample size and the lack of longitudinal data on the within-subject time course of metabolic and cellular dysfunction. Nonetheless, this preliminary report showed robust relationships among the structural and functional callosal measures. Consistent with the literature, we showed elevations in Cho throughout the post-acute period, which were not seen in chronic subjects in this cross-sectional study. NAA reductions were also noted in both post-acute and chronic TBI groups compared to healthy controls. Longitudinal studies are currently underway in our laboratory to confirm the time course of these findings in our sample of moderate-to-severe pediatric TBI patients.

This is the first study to our knowledge that uses multimodal structural and functional correlates specific to the CC. Only post-acute cross-sectional data were available for the correlational analyses, which showed that reductions in NAA were correlated with deficits in general neurocognitive and structural indicators of white matter or axonal integrity (DTI FA). In contrast, elevations in Cho were inversely related to the above functional and structural measures, also in the post-acute period. Multimodal studies focusing on distinct time points and specific brain structures are necessary to delineate the course of the degenerative and reparative processes that occur following a brain injury in childhood to guide the development of targeted therapeutic agents.

Acknowledgments

This work was supported by the National Institutes of Health/National Institute of Neurological Disorders and Stroke (F32NS053169, NS27544, and NS057420), the UCLA Brain Injury Research Center (BIRC), the Della Martin Foundation, and the Winokur Family Foundation/Child Neurology Foundation.

Author Disclosure Statement

No competing financial interests exist.

References

Akpinar, E., Koroglu, M., and Ptak, T. (2007). Diffusion tensor MR imaging in pediatric head trauma. J. Comput. Assist. Tomogr. 31, 657–661.

Arfanakis, K., Haughton, V.M., Carew, J.D., Rogers, B.P., Dempsey, R.J., and Meyerand, M.E. (2002). Diffusion tensor MR imaging in diffuse axonal injury. AJNR Am. J. Neuroradiol. 23, 794–802.

Ashwal, S., Babikian, T., Gardner-Nichols, J., Freier, M.C., Tong, K.A., and Holshouser, B.A. (2006a). Susceptibility-weighted imaging and proton magnetic resonance spectroscopy in assessment of outcome after pediatric traumatic brain injury. Arch. Phys. Med. Rehabil. 87, S50–S58.

Ashwal, S., Holshouser, B.A., Shu, S.K., Simmons, P.L., Perkin, R.M., Tomasi, L.G., Knierim, D.S., Sheridan, C., Craig, K., Andrews, G.H., and Hinshaw, D.B. (2000). Predictive value of proton magnetic resonance spectroscopy in pediatric closed head injury. Pediatr. Neurol. 23, 114–125.

Ashwal, S., Holshouser, B.A., and Tong, K.A. (2006b). Use of advanced neuroimaging techniques in the evaluation of pediatric traumatic brain injury. Dev. Neurosci. 28, 309–326.

Babikian, T., Freier, M.C., Ashwal, S., Riggs, M.L., Burley, T., and Holshouser, B.A. (2006). MR spectroscopy: predicting long-term neuropsychological outcome following pediatric TBI. J. Magn. Reson. Imaging 24, 801–811.

Brenner, T., Freier, M.C., Holshouser, B.A., Burley, T., and Ashwal, S. (2003). Predicting neuropsychologic outcome after traumatic brain injury in children. Pediatr. Neurol. 28, 104–114.

Brown, W.S., Jeeves, M.A., Dietrich, R., and Burnison, D.S. (1999). Bilateral field advantage and evoked potential interhemispheric transmission in commissurotomy and callosal agenesis. Neuropsychologia 37, 1165–1180.

Brown, W.S. (1991). The Bimanual Coordination Test. Unpublished manuscript.

Cecil, K.M., Hills, E.C., Sandel, M.E., Smith, D.H., McIntosh, T.K., Mannon, L.J., Sinson, G.P., Bagley, L.J., Grossman, R.I., and Lenkinski, R.E. (1998). Proton magnetic resonance spectroscopy for detection of axonal injury in the splenium of the corpus callosum of brain-injured patients. J. Neurosurg. 88, 795–801.

Cohen, M. (1997). Children's Memory Scale (CMS). San Antonio: The Psychological Corporation.

Copeland, S., Cazalis, F., Babikian, T., Giza, C.C., Hovda, D.A., and Asarnow, R.F. (2008). A longitudinal DTI study of recovery after traumatic brain injury in adolescents. Paper presented at the UC Neurotrauma Conference, Carmel, CA.

DeBoard Marion, S., Babikian, T., Newman, N., Brown, W., Giza, C., and Asarnow, R.F. (2008). Functional disconnection as measured by interhemispheric communication. Paper presented at the UC Neurotrauma Conference, Carmel, CA.

Delis, D., Kramer, J.H., Kaplan, E., and Ober, B.A. (1994). California Verbal Learning Test–Children's Version (CVLT-C). San Antonio, TX: The Psychological Corporation.

Delis, D., Kramer, J.H., Kaplan, E., and Ober, B.A. (2000). California Verbal Learning Test–Second Edition (CVLT-II). San Antonio, TX: The Psychological Corporation.

Ewing-Cobbs, L., Hasan, K.M., Prasad, M.R., Kramer, L., and Bachevalier, J. (2006). Corpus callosum diffusion anisotropy correlates with neuropsychological outcomes in twins discordant for traumatic brain injury. AJNR Am. J. Neuroradiol. 27, 879–881.

Gentry, L.R., Godersky, J.C., and Thompson, B. (1988). MR imaging of head trauma: review of the distribution and radiopathologic features of traumatic lesions. AJR Am. J. Roentgenol. 150, 663–672.

Gorrie, C., Oakes, S., Duflou, J., Blumbergs, P., and Waite, P.M. (2002). Axonal injury in children after motor vehicle crashes:

extent, distribution, and size of axonal swellings using beta-APP immunohistochemistry. J. Neurotrauma 19, 1171–1182.

Holshouser, B.A., Ashwal, S., Shu, S., and Hinshaw, D.B., Jr. (2000). Proton MR spectroscopy in children with acute brain injury: comparison of short and long echo time acquisitions. J. Magn. Reson. Imaging 11, 9–19.

Holshouser, B.A., Tong, K.A., and Ashwal, S. (2005). Proton MR spectroscopic imaging depicts diffuse axonal injury in children with traumatic brain injury. AJNR Am. J. Neuroradiol. 26, 1276–1285.

Hoon, A.H., Jr., and Melhem, E.R. (2000). Neuroimaging: applications in disorders of early brain development. J. Dev. Behav. Pediatr. 21, 291–302.

Huisman, T.A., Schwamm, L.H., Schaefer, P.W., Koroshetz, W.J., Shetty-Alva, N., Ozsunar, Y., Wu, O., and Sorensen, A.G. (2004). Diffusion tensor imaging as potential biomarker of white matter injury in diffuse axonal injury. AJNR Am. J. Neuroradiol. 25, 370–376.

Hunter, J.V., Thornton, R.J., Wang, Z.J., Levin, H.S., Roberson, G., Brooks, W.M., and Swank, P.R. (2005). Late proton MR spectroscopy in children after traumatic brain injury: correlation with cognitive outcomes. AJNR Am. J. Neuroradiol. 26, 482–488.

Jeeves, M.A., Silver, P.H., and Jacobson, I. (1988). Bimanual coordination in callosal agenesis and partial commissurotomy. Neuropsychologia 26, 833–850.

Jones, D.K. (2004). The effect of gradient sampling schemes on measures derived from diffusion tensor MRI: a Monte Carlo study. Magn. Reson. Med. 51, 807–815.

Levin, H.S., Benavidez, D.A., Verger-Maestre, K., Perachio, N., Song, J., Mendelsohn, D.B., and Fletcher, J.M. (2000). Reduction of corpus callosum growth after severe traumatic brain injury in children. Neurology 54, 647–653.

Mendelsohn, D.B., Levin, H.S., Harward, H., and Bruce, D. (1992). Corpus callosum lesions after closed head injury in children: MRI, clinical features and outcome. Neuroradiology 34, 384–388.

Meythaler, J.M., Peduzzi, J.D., Eleftheriou, E., and Novack, T.A. (2001). Current concepts: diffuse axonal injury-associated traumatic brain injury. Arch. Phys. Med. Rehabil. 82, 1461–1471.

O'Neill, J., Tseng, P.B., Pagare, R., Frew, A.J., Tafazoli, S., and Alger, J.R. (2006). MRSI Voxel Picker (MVP): Software for co-evaluation of structural and spectroscopic information. Paper presented at the ISMRM workshop on Quantitative Spectroscopy.

Parry, L., Shores, A., Rae, C., Kemp, A., Waugh, M.C., Chaseling, R., and Joy, P. (2004). An investigation of neuronal integrity in severe paediatric traumatic brain injury. Child Neuropsychology 10, 248–261.

Preilowski, B.F. (1972). Possible contribution of the anterior forebrain commissures to bilateral motor coordination. Neuropsychologia 10, 267–277.

Provencher, S.W. (2001). Automatic quantitation of localized in vivo 1H spectra with LCModel. NMR Biomed. 14, 260–264.

Ross, B.D., Ernst, T., Kreis, R., Haseler, L.J., Bayer, S., Danielsen, E., Bluml, S., Shonk, T., Mandigo, J.C., Caton, W., Clark, C., Jensen, S.W., Lehman, N.L., Arcinue, E., Pudenz, R., and Shelden, C.H. (1998). 1H MRS in acute traumatic brain injury. J. Magn. Reson. Imaging 8, 829–840.

Rugg, M.D., Milner, A.D., and Lines, C.R. (1985). Visual evoked potentials to lateralised stimuli in two cases of callosal agenesis. J. Neurol. Neurosurg. Psychiatry 48, 367–373.

Sutton, L.N., Wang, Z., Duhaime, A.C., Costarino, D., Sauter, R., and Zimmerman, R. (1995). Tissue lactate in pediatric head trauma: a clinical study using 1H NMR spectroscopy. Pediatr. Neurosurg. 22, 81–87.

Tasker, R.C., Morris, K.P., Forsyth, R.J., Hawley, C.A., and Parslow, R.C. (2006). Severe head injury in children: emergency access to neurosurgery in the United Kingdom. Emerg. Med. J. 23, 519–522.

Tong, K.A., Ashwal, S., Holshouser, B.A., Nickerson, J.P., Wall, C.J., Shutter, L., Osterdock, R.J., Haacke, E.M., and Kido, D.K. (2004). Diffuse axonal injury in children: Clinical correlation with hemorrhagic lesions. Ann. Neurol. 56, 36–50.

Vagnozzi, R., Signoretti, S., Tavazzi, B., Floris, R., Ludovici, A., Marziali, S., Tarascio, G., Amorini, A.M., Di Pietro, V., Delfini, R., and Lazzarino, G. (2008). Temporal window of metabolic brain vulnerability to concussion: a pilot 1H-magnetic resonance spectroscopic study in concussed athletes—part III. Neurosurgery 62, 1286–1295; discussion 1295–1286.

Walz, N.C., Cecil, K.M., Wade, S.L., and Michaud, L.J. (2008). Late proton magnetic resonance spectroscopy following traumatic brain injury during early childhood: relationship with neurobehavioral outcomes. J. Neurotrauma 25, 94–103.

Wechsler, D. (1999). Wechsler Abbreviated Intelligence Scale (WASI). San Antonio, TX: The Psychological Corporation.

Wechsler, D. (1997). Wechsler Adult Intelligence Scale–Third Edition (WAIS-III). San Antonio, TX: The Psychological Corporation.

Wechsler, D. (2003). Wechsler Intelligence Scale for Children–Fourth Edition (WISC-IV). San Antonio, TX: The Psychological Corporation.

Wechsler, D. (1977). Wechsler Memory Scale Third Edition (WMS-III). San Antonio, TX: The Psychological Corporation.

Wilde, E.A., Chu, Z., Bigler, E.D., Hunter, J.V., Fearing, M.A., Hanten, G., Newsome, M.R., Scheibel, R.S., Li, X., and Levin, H.S. (2006). Diffusion tensor imaging in the corpus callosum in children after moderate to severe traumatic brain injury. J Neurotrauma 23, 1412–1426.

Yeo, R.A., Phillips, J.P., Jung, R.E., Brown, A.J., Campbell, R.C., and Brooks, W.M. (2006). Magnetic resonance spectroscopy detects brain injury and predicts cognitive functioning in children with brain injuries. J. Neurotrauma 23, 1427–1435.

Yuan, W., Holland, S.K., Schmithorst, V.J., Walz, N.C., Cecil, K.M., Jones, B.V., Karunanayaka, P., Michaud, L., and Wade, S.L. (2007). Diffusion tensor MR imaging reveals persistent white matter alteration after traumatic brain injury experienced during early childhood. AJNR Am. J. Neuroradiol. 28, 1919–1925.

Address correspondence to:
Talin Babikian, Ph.D., M.P.H.
Semel Institute for Neuroscience and Human Behavior
Psychiatry and Biobehavioral Sciences
David Geffen School of Medicine
University of California–Los Angeles
760 Westwood Plaza, Room C8-746
Los Angeles, CA 90095

E-mail: tbabikian@mednet.ucla.edu